Inorg. Chem. **2006**, *45*, 10670–10677

Synthesis and Spectroscopic Properties of Platinum(II) Terpyridine Complexes Having an Arylborane Charge Transfer Unit

Eri Sakuda, Akiko Funahashi, and Noboru Kitamura*

Division of Chemistry, Graduate School of Science, Hokkaido University, Sapporo 060-0810, Japan

Received July 31, 2006

Synthesis, redox, spectroscopic, and photophysical properties of a new class of Pt(II) complexes of the type $[PtL_n\text{-}Cl]^+$ are reported, where L_n is 4′-phenyl(dimesitylboryl)-2,2′:6′,2″-terpyridine (L_1) or 4′-duryl(dimesitylboryl)-2,2′:6′,2″-terpyridine (L_2). The free L_1 or L_2 ligand in CH_3CN shows the absorption band responsible for intramolecular charge transfer (CT) from the π-orbital of the aryl group in L_1 or L_2 (π(aryl)) to the vacant p-orbital on the boron atom (p(B)), in addition to $\pi\pi^*$ absorption in the 2,2′:6′,2″-terpyridine (tpy) unit. In particular, the L_1 ligand shows an intense CT absorption band as compared with L_2. Such intramolecular π(aryl)–p(B) CT interactions in L_1 give rise to large influences on the redox, spectroscopic, and photophysical properties of $[PtL_1Cl]^+$. In practice, $[PtL_1Cl]^+$ shows strong room-temperature emission in $CHCl_3$ with the quantum yield and lifetime of 0.011 and 0.6 μs, respectively, which has been explained by synergetic effects of Pt(II)-to-L_1 MLCT and π(aryl)–p(B) CT interactions on the electronic structures of the complex. In the case of $[PtL_2Cl]^+$, the dihedral angle between the planes produced by the tpy and duryl(dimesitylborane) groups is very large (84°) as compared with that between the tpy and phenyl-(dimesitylborane) units in $[PtL_1Cl]^+$ (26–39°), which disturbs electron communication between the Pt(II)–tpy and arylborane units in $[PtL_2Cl]^+$. Thus, $[PtL_2Cl]^+$ is nonemissive at room temperature. The important roles of the synergetic CT interactions in the excited-state properties of the $[PtL_1Cl]^+$ complex are shown clearly by emission quenching of the complex by a fluoride ion. The X-ray crystal structure of $[PtL_1Cl]^+$ is also reported.

Introduction

The vacant p-orbital on the boron atom (p(B)) in a triarylborane derivative plays crucial roles in determining the electronic structure of the compound. As a typical example, tris(9-anthryl)borane (TAB) first reported by Yamaguchi et al. shows broad and structureless absorption and fluorescence bands in the visible region, which are different totally from those of anthracene itself.[1–4] Our recent studies on the spectroscopic and excited-state properties of TAB indicated that the characteristic absorption and fluorescence bands mentioned above were ascribed essentially to the charge transfer (CT) transition between the π-orbital of the anthryl group (π(aryl)) and p(B): π(aryl)−p(B) CT. In practice, the dipole moment change accompanied by the CT transition in TAB is as large as ∼8.0 D.[5–7] Beside TAB, it has been reported that various triarylborane derivatives show unique spectroscopic properties. Therefore, an appropriate choice of an aryl group(s) in a triarylborane derivative would provide a new class of novel functional materials.

One possible approach to the research along the line mentioned above is to combine a π(aryl)−p(B) system with other electronic system of a molecule.[8] Among various molecular systems, a metal-to-ligand charge transfer (MLCT) system of a transition metal complex has received broad research interests, and its applications to functional materials

* To whom correspondence should be addressed. E-mail: kitamura@sci.hokudai.ac.jp.

(1) Yamaguchi, S.; Akiyama, S.; Tamao, K. *J. Am. Chem. Soc.* **2000**, *122*, 6335.
(2) Yamaguchi, S.; Shirasaka, T.; Tamao, K. *Org. Lett.* **2000**, *2*, 4129.
(3) Yamaguchi, S.; Akiyama, S.; Tamao, K. *J. Am. Chem. Soc.* **2001**, *123*, 11372.
(4) Yamaguchi, S.; Akiyama, S.; Tamao, K. *J. Orgnomet. Chem.* **2002**, *652*, 3.
(5) Kitamura, N.; Sakuda, E. *J. Phys. Chem. A* **2005**, *109*, 7429.
(6) Kitamura, N.; Sakuda, E.; Yoshizawa, T.; Iimori, T.; Ohta, N. *J. Phys. Chem. A* **2005**, *109*, 7435.
(7) Sakuda, E.; Tsuge, K.; Sasaki, Y.; Kitamura, N. *J. Phys. Chem. B* **2005**, *109*, 22326.
(8) (a) Jia, W.-L.; Song, D.-R.; Wang, S. *J. Org. Chem.* **2003**, *68*, 701. (b) Jia, W.-L.; Bai, D.-R.; McCormick, T.; Liu, Q.-D.; Motala, M.; Wang, R.-Y.; Sewawd, C.; Tao, Y.; Wang, S. *Chem. Eur. J.* **2004**, *10*, 994.

10.1021/ic061435b CCC: $33.50
Published on Web 11/29/2006

such as light-emitting diodes and nonlinear optical devices are expanding research areas.[9] Synthetic control of the redox, spectroscopic, and excited-state properties of a transition metal complex is thus the fundamental basis for further advances in the relevant researches, and various studies have been explored by employing a variety of π-chromophoric ligands and transition metal ions: Ru(II);[10−16] Re(I);[17−19] Pt(II);[20−22] Ir(III).[23−24] Among these metal complexes, a square-planar Pt(II) complex is quite interesting, since it shows MLCT, ligand-centered (LC), and/or metal-metal-to-ligand CT (MMLCT) emission, depending on a ligand structure, temperature, medium, or concentration.[25−34] This indicates that the orbital energies involved in the ground and excited states of the complex respond very sensitively to these factors and, thus, synthetic control of redox, spectroscopic, and excited-state properties of a Pt(II) complex is worth exploring.

Our strategy toward tuning the redox, spectroscopic, and excited-state properties of a Pt(II) complex is to combine the π(aryl)−p(B) CT interaction in a triarylborane derivative with the MLCT state of the complex. In the case of a [Pt(ph-tpy)Cl]$^+$ complex (ph-tpy = 4′-phenyl-2,2′:6′,2″-terpyridine), it has been reported that an introduction of an electron donor or acceptor substituent on the phenyl ring in ph-tpy influences the excited-state properties of the complex through variations of both MLCT and d−d excited-state energies.[20−22,29,31,33] An introduction of a triarylborane chromophore to the ligand of a Pt(II) complex would also influence the excited-state properties. We expect, therefore, that π(aryl)−p(B) CT interactions in a triarylborane ligand unit influence the MLCT excited state of a Pt(II) complex, and this provides new and novel characteristics of the complex.

Scheme 1. Synthesis of $[PtL_1Cl]^+$ and $[PtL_2Cl]^+$ Complexes[a]

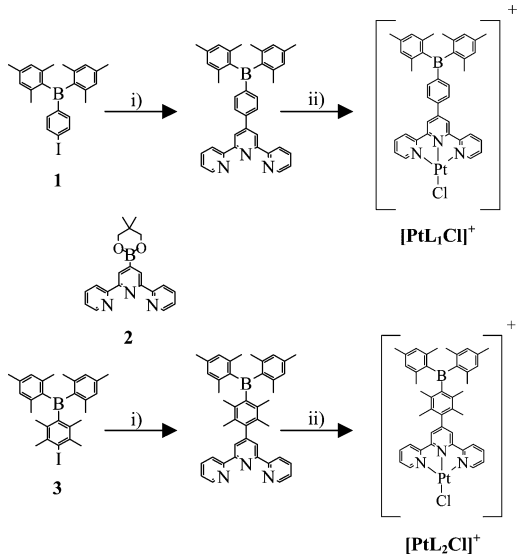

[a] Key: (i) **2**, $Pd(PPh_3)_4$, and Na_2CO_3 in a CH_3CN/THF/EtOH mixture; (ii) $[Pt(COD)Cl_2]$ in MeOH, where COD = 1,5-cyclooctadiene.

As a new ligand, we designed a tpy derivative having a phenyl(dimesitylborane) (L_1) or duryl(dimesitylborane) unit (L_2) at the 4′-position of tpy: the structures are shown in Scheme 1. Since an organic borane derivative is generally moisture sensitive and the periphery of the boron atom in the compound should be surrounded by bulky groups, we introduced mesityl groups on the boron atom in L_1 or L_2. On the basis of such ligand design, L_1/L_2 and their Pt(II) complexes prepared are stable in solution and air. In the following, we report synthesis of the L_1 and L_2 ligands, and their Pt(II) complexes: $[PtL_1Cl]^+$ and $[PtL_2Cl]^+$. Characteristic redox, spectroscopic (absorption and emission), and excited-state properties of $[PtL_1Cl]^+$ and $[PtL_2Cl]^+$ in CH_3CN or $CHCl_3$ are reported. On the basis of the present results, we discuss the roles of the π(aryl)−p(B) CT interactions in the MLCT excited state of the complex. The X-ray crystal structure of $[PtL_1Cl]^+$ is also reported.

Experimental Section

Chemicals. Tetrakis(triphenylphosphine)palladium(0) ($Pd(PPh_3)_4$, Tokyo Kasei Kogyo Co., Ltd.), potassium tetrachloroplatinate(II) ($K_2[Pt^{II}Cl_4]$, Wako Pure Chemicals Ind), and 1,5-cyclooctadiene (COD, Wako Pure Chemicals Ind) were used as supplied. Acetonitrile (Wako Pure Chemicals Ind), *N*,*N*-dimethylformamide (DMF, Kanto Chemical Co. Inc.), and tetra-*n*-butylammonium perchlorate (Wako Pure Chemicals Ind) for spectroscopic and/or electrochemi-

(9) For instance; (a) Bouder, T. L.; Maury, O.; Bondon, A.; Costuas, K.; Amouyal, E.; Ledoux, I.; Zyss, J.; Bozec, H. L. *J. Am. Chem. Soc.* **2003**, *125*, 12284. (b) Coe, B. J.; Harris, J. A.; Brunschwig, B. S.; Asselberghs, I.; Clays, K.; Garin, J.; Orduna, J. *J. Am. Chem. Soc.* **2005**, *127*, 13399.
(10) Rillema, D. P.; Allen, G.; Meyer, T. J.; Conrad, D. *Inorg. Chem.* **1983**, *22*, 1617.
(11) Caspar, J. V.; Meyer, T. J. *Inorg. Chem.* **1983**, *22*, 2444.
(12) Allen, G. H.; White, R. P.; Rillema, D. P.; Meyer, T. J. *J. Am. Chem. Soc.* **1984**, *106*, 2613.
(13) Ohsawa, Y.; Hanck, K. W.; DeArmond, M. K. *J. Electroanal. Chem.* **1984**, *175*, 229.
(14) Dodsworth, E. S.; Lever, A. B. P. *Chem. Phys. Lett.* **1985**, *119*, 61.
(15) Kawanishi, Y.; Kitamura, N.; Tazuke, S. *Inorg. Chem.* **1989**, *28*, 2968.
(16) For recent reviews, see: Wang, X.-Y.; Guerzo, A. D.; Schmehl, R. H. *J. Photochem. Photobiol., C* **2004**, *5*, 55.
(17) Caspar, J. V.; Sullivan, B. P.; Meyer, T. J. *Inorg. Chem.* **1984**, *23*, 2104.
(18) Juris, A.; Campagna, S.; Bidd, I.; Lehn, J.-M.; Ziessel, R. *Inorg. Chem.* **1988**, *27*, 4007.
(19) Wallace, L.; Rillema, D. P. *Inorg. Chem.* **1993**, *32*, 3836.
(20) Michalec, J. F.; Bejune, S. A.; McMillin, D. R. *Inorg. Chem.* **2000**, *39*, 2708.
(21) Michalec, J. F.; Bejune, S. A.; Cuttell, D. G.; Summerton, G. C.; Gertenbach, J. A.; Field, J. S.; Haines, R. J.; McMillin, D. R. *Inorg. Chem.* **2001**, *40*, 2193.
(22) McMillin, D. R.; Moore, J. J. *Coord. Chem. Rev.* **2002**, *229*, 113.
(23) Lamansky, S.; Djurovich, P.; Murphy, D.; Abdel-Razzaq, F.; Lee, H.-E.; Adachi, C.; Burrows, P. E.; Forrest, S. R.; Thompson, M. E. *J. Am. Chem. Soc.* **2001**, *123*, 4304.
(24) Beeby, A.; Bettington, S.; Samuel, I. D. W.; Wang, Z. *J. Mater. Chem.* **2003**, *13*, 80.
(25) Aldridge, T. K.; Stacy, E. M.; McMillin, D. R. *Inorg. Chem.* **1994**, *33*, 722.
(26) Bailey, J. A.; Hill, M. G.; Marsh, R. E.; Miskowski, V. M.; Schaefer, W. P.; Gray, H. B. *Inorg. Chem.* **1995**, *34*, 4591.
(27) Hill, M. G.; Bailey, J. A.; Miskowski, V. M.; Gray, H. B. *Inorg. Chem.* **1996**, *35*, 4585.
(28) Büchner, R.; Field, J. S.; Haines, R. J.; Cunningham, C. T.; McMillin, D. R. *Inorg. Chem.* **1997**, *36*, 3952.
(29) Arena, G.; Calogero, G.; Campagna, S.; Scolaro, L. M.; Ricevuto, V.; Romeo, R. *Inorg. Chem.* **1998**, *37*, 2763.
(30) Crites, D. K.; Cunningham, C. T.; McMillin, D. R. *Inorg. Chim. Acta* **1998**, *273*, 346.
(31) Büchner, R.; Cunningham, C. T.; Field, J. S.; Haines, R. J.; McMillin, D. R.; Summerton, G. C. *J. Chem. Soc., Dalton Trans.* **1999**, 711.
(32) Hobert, S. E.; Carney, J. T.; Cummings, S. D. *Inorg. Chim. Acta* **2001**, *318*, 89.
(33) Field, J. S.; Haines, R. J.; McMillin, D. R.; Summerton, G. C. *J. Chem. Soc., Dalton Trans.* **2002**, 1369.
(34) Guo, F.; Sun, W.; Liu, Y.; Schanze, K. *Inorg. Chem.* **2005**, *44*, 4055.

cal measurements were purified by the accepted procedures prior to use.[35] Tetra-*n*-butylammonium fluoride (TBAF, Wako Pure Chemicals Ind) was purified by repeated recrystallizations from an acetone/diethyl ether mixture. Other chemicals used in this study were the highest grade available from domestic suppliers and used without further purification.

Synthesis of Boron-Containing Terpyridine Ligands and Their Pt(II) Complexes. 4′-Phenyl(dimesitylboryl)-2,2′;6′,2″-terpyridine (L_1), 4′-duryl(dimesitylboryl)-2,2′;6′,2″-terpyridine (L_2), and their platinum(II) complexes were synthesized according to Scheme 1. Detailed synthetic procedures are as follows.

4′-Phenyl(dimesitylboryl)-2,2′:6′,2″-terpyridine (L_1). A tetrahydrofuran (THF, 3 mL) solution of (iodophenyl)dimesitylborane (**1**, 450 mg, 1.0 mM)[2] and $Pd(PPh_3)_4$ (45 mg) was deaerated by purging an N_2-gas stream for 10 min under stirring. Into the solution, 4′-((neopentyl glycolato)boron)-2,2′:6′,2″-terpyridine (**2**, 0.17 g, 0.5 mM)[36] dissolved in a CH_3CN (10 mL)/THF (15 mL)/EtOH (15 mL) mixture and an aqueous Na_2CO_3 solution (2 M, 0.62 mL) were added.[37] The mixture was deaerated by purging an N_2-gas stream for 10 min and, then, heated at reflux (85 °C) for 6 h under N_2 atmosphere. After complete consumption of **2** as confirmed by thin-layer chromatography, the solvents were removed under reduced pressure. The residues dissolved in CH_2Cl_2 (25 mL) were washed successively with H_2O (25 mL) and a dilute aqueous NaOH solution (0.1 M, 100 mL) for three times and dried over anhydrous Na_2SO_4. Removal of the solvents gave colorless solids. The crude product was purified by column chromatography on deactivated alumina with an ethyl acetate/*n*-hexane (1:9, v/v %) mixture as an eluent: colorless powder (yield = 29%). ^{1}H NMR (270 MHz, $CDCl_3$): δ 8.74 (s, 4H), 8.72 (m, 2H), 8.68 (d, 2H, J = 8 Hz), 7.89 (t, 2H, J = 8 Hz, 8 Hz), 7.83 (d, 2H, J = 8 Hz) 7.64 (d, 2H, J = 8 Hz), 7.36 (m, 2H), 6.85 (s, 4H), 2.33 (s, 6H), 2.04 (s, 12H). MS (FD-MS): m/z 557 (M^+).

4′-Duryl(dimesitylboryl)-2,2′:6′,2″-terpyridine (L_2). The L_2 ligand was synthesized by the procedures analogous to those of L_1. A THF solution (3 mL) of **1** (380 mg, 8.3 mM)[2] and $Pd(PPh_3)_4$ (45 mg) was deaerated by purging an N_2-gas stream for 10 min under stirring. Into the solution, **2** (0.17 g, 0.5 mM) dissolved in a CH_3CN (10 mL)/THF (15 mL)/EtOH (10 mL) mixture and an aqueous Na_2CO_3 solution (2 M, 0.62 mL) were added. The mixture was deaerated by purging an N_2-gas stream for 10 min and then heated at reflux (85 °C) for 8 h under N_2 atmosphere. Workup procedures analogous to those for preparation of L_1 gave a dark-yellow powder (yield = 48%). ^{1}H NMR (270 MHz, DMSO-d_6): δ 8.71 (d, 2H), 8.66 (br, 2H), 8.59 (d, 2H), 7.87 (dt, 2H), 7.36 (dt, 2H), 6.73 (s, 4H), 2.44 (br, 6H), 2.26 (br, 6H), 2.09 (br, 6H), 1.98 (br, 12H).[38] MS (FD-MS): m/z 613 (M^+).

$[PtL_1Cl]^+PF_6^-$/$[PtL_2Cl]^+PF_6^-$. Into a suspension of $[Pt(COD)Cl_2]$ (0.15 g, 0.4 mmol)[39] in methanol (25 mL), solid L_1 or L_2 (0.45 mM) was added under stirring and the mixture was heated at 60 °C. After 2 h reaction, all of the solid reactants were dissolved and the mixture turned to a clear yellow solution. After cooling of the sample to room temperature, unreacted $[Pt(COD)Cl_2]$ precipitated was removed by filtration. The filtrate was then evaporated to dryness, giving red-orange solids. The solids were washed thoroughly with diethyl ether and then dissolved in a small amount of methanol. Into the solution, an excess amount of a methanol solution of NH_4PF_6 was added. The PF_6 salt precipitated was collected by suction filtration and recrystallized from acetone, affording a pure product: yellow crystal ($[PtL_1Cl]^+PF_6^-$) or red powder ($[PtL_2Cl]^+PF_6^-$), yield = 53 or 73%, respectively.

(i) $[PtL_1]^+PF_6^-$. ^{1}H NMR (270 MHz, DMSO-d_6): δ 9.04 (s, 2H), 8.99 (br, 2H), 8.87 (d, 2H, J = 8 Hz), 8.57 (m, 2H), 8.15 (d, 2H, J = 8 Hz), 8.00 (m, 2H), 7.61 (d, 2H, J = 9 Hz), 6.88 (s, 4H), 2.29 (s, 6H), 1.98 (s, 12H). MS (ESI-HRMS): m/z 787.23 (M^+-PF_6). Anal. Calcd for $C_{39}H_{36}BN_3PtClPF_6$: C, 50.20; H, 3.89; N, 4.50. Found: C, 50.28; H, 4.13; N, 4.30.

(ii) $[PtL_2]^+PF_6^-$.[40] 1H NMR (DMSO-d_6, 270 MHz): δ 9.02 (d, 2H, J = 4 Hz), 8.79 (d, 2H, J = 8 Hz), 8.57 (s, 2H), 8.52 (t, 2H, J = 7 Hz, 8 Hz), 7.99 (t, 2H, J = 6 Hz, 6 Hz), 6.82 (s, 4H), 2.25 (s, 6H), 2.03 (s, 12H), 1.95 (s, 12H). MS (ESI-HRMS): m/z 843.96 (M^+ $^-$ PF_6).

Spectroscopic and Electrochemical Measurements. Absorption and corrected emission spectra of the complexes at 298 K were recorded on a Hitachi UV-3300 spectrophotometer and a Hitachi F-4500 spectrofluorometer, respectively. The emission quantum yields (Φ^{em}) of the Pt(II) complexes were determined by using $[Ru(bpy)_3](PF_6)_2$ in CH_3CN as a standard (0.061).[41] Emission lifetime measurements were conducted by using a streak camera (Hamamatsu Photonics, C4334) as a photodetector at 355 nm excitation (Continuum Surelite-II, 355 nm, 6 ns pulse width). For emission spectroscopy, sample solutions were deaerated by purging an Ar-gas stream over 30 min. NMR spectra were recorded on a JEOL JME-EX270 FT-NMR SYSTEM (270 MHz).

Cyclic voltammetry was conducted by using an electrochemical analyzer (BAS, ALS-701A). The concentration of the Pt complex in DMF was set at 5×10^{-4} M, and tetra-*n*-butylammonium perchlorate ($TBAClO_4$, 0.1 M) was used as a supporting electrolyte. The solution was deaerated by purging an Ar-gas stream over 20 min prior to the experiments. A three-electrode system was employed by using platinum working, platinum auxiliary, and SCE reference electrodes.

Crystallography. The X-ray structural data for single $[PtL_1Cl]^+PF_6^-$ crystals were collected on Mercury CCD area detectors coupled with Rigaku AFC-7R diffractometers, by using CrystalClear (Rigaku Co.) with graphite-monochromated Mo Kα radiation (0.7107 Å). The structures were solved by CrystalStructure 3.6.0[42] and SHELX97.[43] Full-matrix least-square refinements were employed against F^2. Crystallographic data (excluding structure factors) for the structure reported in this paper have been deposited with Cambridge Crystallographic Data Center as supplementary publication no. CCDC-170237. Copies of the data can be obtained free of charge on application to CCDC, 12 Union Road, Cambridge CB2 1EZ, U.K. (fax, (+44) 1223-336-033; e-mail, deposit@ccdc.cam.ac.uk).

Results and Discussion

X-ray Crystal Structure of $[PtL_1Cl](PF_6)$. Recrystallizations of $[PtL_1Cl]^+$ from acetone gave yellow single crystals, and we conducted an X-ray crystal structure analysis of the

(35) Perrin, D. D.; Armarego, W. L. F.; Perrin, D. R. *Purification of Laboratory Chemicals*, 2nd ed.; Pergamon Press: New York, 1980.
(36) Aspley, C. J.; Williams, J. A. G. *New J. Chem.* **2001**, *25*, 1136.
(37) Goodall, W.; Wild, K.; Arm, K. J.; Williams, J. A. G. *J. Chem. Soc., Perkin Trans. 2* **2002**, 1669.
(38) Since the NMR spectrum was very complicated, we have not determined the *J* values.
(39) McDermott, J. X.; White, J. F.; Whitesides, G. M. *J. Am. Chem. Soc.* **1976**, *98*, 6521.
(40) Elemental analysis suggests that the complex includes a small amount of an impurity, which cannot be detected by the NMR/mass spectra and the cyclic voltammogram of the complex. However, this does not influence the main conclusions of this study: participation of the synergetic MLCT/π(aryl)−p(B) CT interactions in $[PtL_1Cl]^+$.
(41) Caspar, J. V.; Meyer, T. J. *J. Am. Chem. Soc.* **1983**, *105*, 5583.
(42) *Crystal Structure Analysis Package*; Rigaku and Rigaku/MSC: 9009 NewTrails Dr., The Woodlands, TX 77381, 2000−2004.
(43) Sheldrick, G. M. *A program for crystal structure determination and refinement*; University of Göttingen: Göttingen, Germany, 1997.

Table 1. Crystallographic Data for $[PtL_1Cl]^+$ Crystals[a]

formula	$C_{42}H_{42}N_3OPtBPF_6Cl$
fw	991.13
size, mm	$0.13 \times 0.13 \times 0.03$
T, K	153.1
cryst syst	triclinic
space group	$P\bar{1}$
cell constants	
a, Å	9.220(3)
b, Å	12.734(4)
c, Å	17.939(5)
α, deg	101.335(3)
β, deg	90.097(4)
γ, deg	101.769(4)
V, Å^3	2019.8(10)
Z	2
ρ_{calc}, g/cm^3	1.630
μ, cm^{-1}	36.30
λ(Mo Kα), Å	0.7107
$R1$, %	0.041
$wR2$, %	0.105

[a] $R1 = \Sigma||F_o| - |F_c||/\Sigma|F_o|$, $wR2 = [\Sigma(|F_o| - |F_c|)^2/\Sigma w|F_o|^2]^{1/2}$.

Table 2. Selected Bond Distances/angles for $[PtL_1Cl]^+$

atoms	distance (Å)	atoms	distance (Å)
Pt(1)−Cl(1)	2.290(2)	C(8)−C(16)	1.482(8)
Pt(1)−N(1)	2.020(4)	C(19)−B(1)	1.572(9)
Pt(1)−N(2)	1.948(4)	C(22)−B(1)	1.569(9)
Pt(1)−N(3)	2.017(4)	C(31)−B(1)	1.596(7)

atoms	angle (deg)	atoms	angle (deg)
N(1)−Pt(1)−Cl(1)	98.9(1)	C(18)−C(19)−B(1)	121.8(5)
N(2)−Pt(1)−Cl(1)	178.9(1)	B(1)−C(19)−C(20)	121.7(4)
N(3)−Pt(1)−Cl(1)	99.1(1)	C(19)−B(1)−C(22)	120.0(4)
N(2)−Pt(1)−N(1)	81.1(2)	C(19)−B(1)−C(31)	116.5(5)
N(3)−Pt(1)−N(2)	80.9(2)	B(1)−C(22)−C(23)	122.0(6)
N(3)−Pt(1)−N(1)	162.0(2)	B(1)−C(22)−C(27)	120.8(5)
C(7)−C(8)−C(16)	120.4(5)	C(22)−B(1)−C(31)	123.4(5)
C(16)−C(8)−C(9)	121.3(4)	B(1)−C(31)−C(32)	119.8(5)
C(8)−C(16)−C(17)	120.8(4)	C(31)−C(32)−C(33)	119.7(5)
C(8)−C(16)−C(21)	120.0(5)	B(1)−C(31)−C(36)	121.5(5)

complex. Tables 1 and 2 summarize the crystallographic data and selected bond distances/angles of $[PtL_1Cl]^+$, respectively. Figure 1 also shows the molecular structure of the complex determined by X-ray crystallography.

The carbon (C)−boron (B)−carbon (C) bond angles (angle C−B−C) of the phenyl(dimesitylborane) unit in the complex are ca. 120° (116.5(5), 120.0(4), and 123.4(5)°). This is readily understood by the sp^2-like configuration of the boron atom. On the other hand, the bond distances and angles of the Pt−tpy unit are comparable to those of $[Pt(tpy)Cl]^+$[27] and the Cl−Pt(II)−tpy plane is almost planar similar to that of $[Pt(ph\text{-}tpy)Cl]^+$.[21,31] Therefore, an introduction of the phenyl(dimesitylborane) group to the 4′-position of tpy does not influence the coordination structure of the complex around the Pt ion. X-ray structure analysis of the complex demonstrates, however, that the dihedral angle between the Cl−Pt(II)−tpy and phenyl planes is 26°: see Figure 1. Such a geometrical distortion (i.e., non-coplanarity) has been also reported for $[Pt(ph\text{-}tpy)Cl]^+$ and is responsible for steric hindrance between the hydrogen atoms in the tpy and phenyl groups in the complex. In the case of $[PtL_2Cl]^+$, this indicates that the dihedral angle between the tpy and duryl planes should be much larger than that of $[PtL_1Cl]^+$, owing to large steric hindrance between the methyl groups in the duryl unit

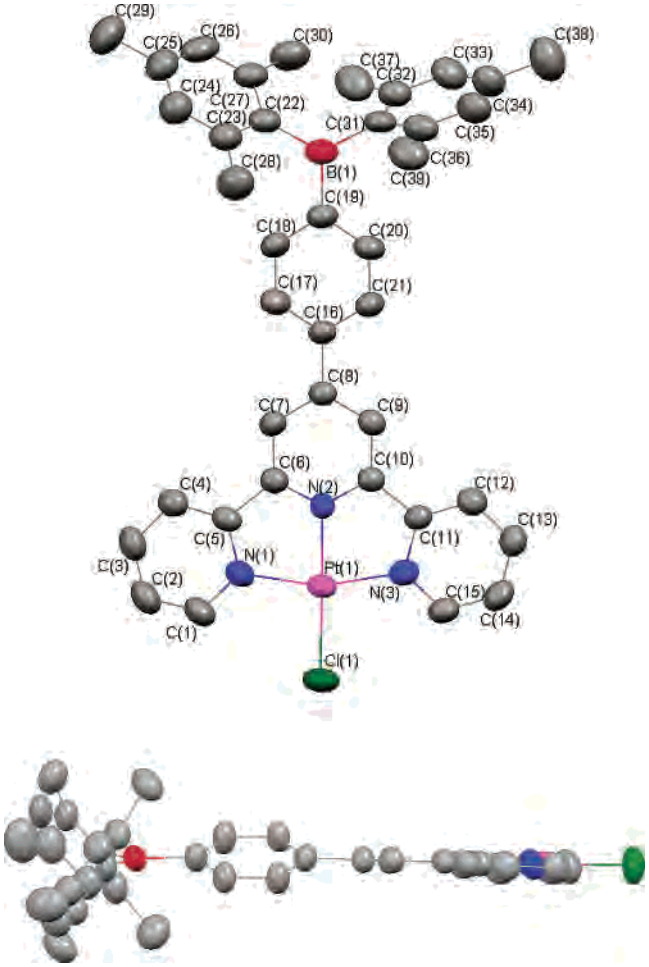

Figure 1. X-ray crystal structures of $[PtL_1Cl]^+$.

and the hydrogen atoms in tpy. Unfortunately, we have not obtained single crystals of $[PtL_2Cl]^+$ and, thus, the crystal structure of the complex is unknown at the present stage of the investigation. Nonetheless, our molecular orbital calculations (WinMOPAC/AM 1) on the L_1 and L_2 ligands (not Pt complexes) indicate that the dihedral angle between the tpy and phenyl (L_1) or duryl planes (L_2) is 39 or 84°, respectively. The dihedral angle calculated for L_1 (39°) is comparable to that determined by X-ray crystallography for $[PtL_1Cl]^+$: 26°. These discussions indicate that the dihedral angle between the tpy and duryl planes in $[PtL_2Cl]^+$ could be much larger than that of $[PtL_1Cl]^+$, which should reflect on other physical properties of the complexes. In practice, such structural differences reflected on the redox, spectroscopic, and excited-state properties of the $[PtL_1Cl]^+$ and $[PtL_2Cl]^+$ complexes as described in the following sections.

Redox Properties of $[PtL_1Cl]^+$ and $[PtL_2Cl]^+$. Figure 2 shows cyclic voltammograms of the Pt(II) complexes in DMF. An irreversible oxidation peak is observed for $[Pt(tpy)Cl]^+$ at around 1.0 V (vs SCE), while oxidation of $[PtL_2Cl]^+$ is ambiguous and no obvious oxidation peak is observed for $[PtL_1Cl]^+$. On the other hand, each complex shows reversible two reduction peaks as the data are summarized in Table 3. Although both the first ($E^{red(1)}$) and second reduction potentials ($E^{red(2)}$) of $[PtL_2Cl]^+$ are almost comparable to those of $[Pt(tpy)Cl]^+$ at −0.76 to −0.78 and −1.31

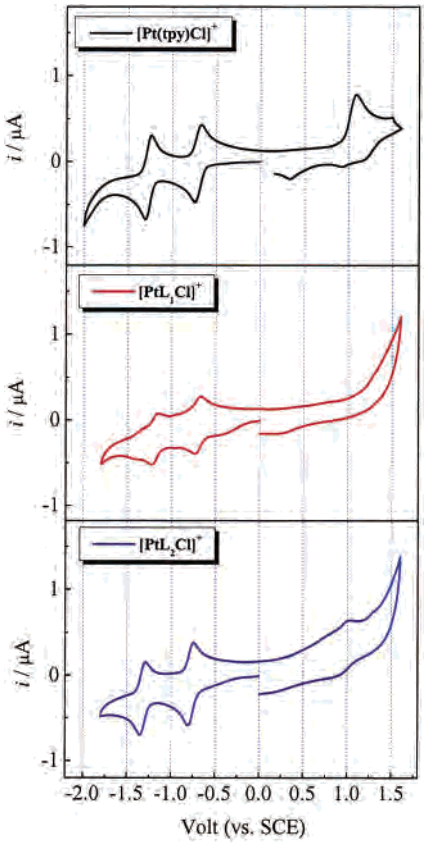

Figure 2. Cyclic voltammograms of the Pt(II) complexes (5×10^{-4} M) in DMF in the presence of 0.1 M (TBA)ClO_4 (scan rate = 100 mV/s).

Table 3. Reduction Potentials of the Pt(II) Complexes

compd	redn potential/V[a] (vs SCE)	
	$E^{red}(1)$	$E^{red}(2)$
$[Pt(tpy)Cl]^+$	−0.76	−1.31
$[PtL_1Cl]^+$	−0.71	−1.19
$[PtL_2Cl]^+$	−0.78	−1.33
[Pt-4′-ph-tpyCl]+ [b]	(−1.22)	(−1.76)

[a] In DMF at 298 K. [b] Data taken from ref 21 reported vs $Fc^{+/0}$ in DMF (0.1 M TBAH).

to −1.33 V (vs SCE), respectively, the potentials of $[PtL_1Cl]^+$ are shifted to the positive direction by 50−70 (−0.71 V) and 120−140 mV (−1.19 V), respectively. In the case of $[Pt(tpy)Cl]^+$, since the lowest excited state is the MLCT state, the first reduction peak of the complex is ascribed to reduction of the tpy ligand. Therefore, the first reduction potential of $[PtL_1Cl]^+$ or $[PtL_2Cl]^+$ could be also assigned to the reduction of the L_1 or L_2 ligand in the complex, respectively. The presence of the four methyl groups in L_2 contributes partly to the negative potential shifts of $[PtL_2Cl]^+$ as compared with the $E^{red(1)}$ and $E^{red(2)}$ values of $[PtL_1Cl]^+$. As discussed in the preceding section, on the other hand, the dihedral angle between the tpy and phenyl planes in $[PtL_1Cl]^+$ is ∼26°. Therefore, electron delocalization would take place more or less over the L_1 ligand in $[PtL_1Cl]^+$, while the large dihedral angle between the tpy and duryl planes (predicted to be 84°) would disturb electron delocalization over the L_2 ligand in $[PtL_2Cl]^+$. We suppose that this will be the primary reason for the positive shifts of the $E^{red(1)}$ and $E^{red(2)}$ values of $[PtL_1Cl]^+$ as compared with the relevant value of $[PtL_2Cl]^+$. The $E^{red(1,2)}$ values of $[PtL_2Cl]^+$ comparable to those of $[Pt(tpy)Cl]^+$ will also support insufficient electron delocalization over the L_2 ligand in the complex. It is worth emphasizing, furthermore, that the vacant p-orbital on the boron atom in a triarylborane derivative shows an electron-withdrawing ability. Therefore, we suppose that the positive shifts of $E^{red(1)}$ and $E^{red(2)}$ observed for $[PtL_1Cl]^+$ as compared with those of $[PtL_2Cl]^+$ and $[Pt(tpy)Cl]^+$ are responsible essentially for the presence of the phenyl(dimesitylborane) unit in the L_1 ligand and, thus, for the contribution of π(aryl)−p(B) CT interactions to the electronic structure of the $[PtL_1Cl]^+$ complex.

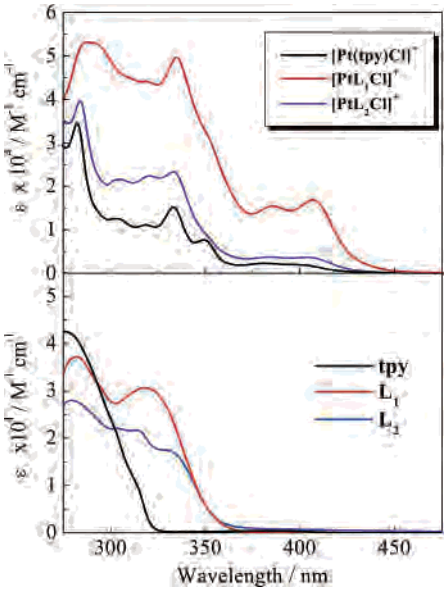

Figure 3. Absorption spectra of the Pt(II) complexes (upper panel) and the free ligands in CH_3CN at 298 K (lower panel).

Electronic Absorption Characteristics of $[PtL_1Cl]^+$ and $[PtL_2Cl]^+$. Aborption spectra of $[PtL_1Cl]^+$ and $[PtL_2Cl]^+$ in CH_3CN at 298 K are shown in Figure 3a, together with that of $[Pt(tpy)Cl]^+$. Figure 3b also shows absorption spectra of L_1, L_2, and tpy in CH_3CN as references, and the spectroscopic data are summarized in Table 4. The absorption bands observed for $[PtL_1Cl]^+$ or $[PtL_2Cl]^+$ at around 400 and 330−290 nm are assigned to the MLCT and LC($\pi\pi^*$) transitions, respectively, as judged from the assignment of the relevant transition in $[Pt(tpy)Cl]^+$. The MLCT absorption maximum wavelength (λ^{abs}) of $[PtL_2Cl]^+$ (404 nm) is almost comparable to that of $[Pt(tpy)Cl]^+$ (402 nm), while that of $[PtL_1Cl]^+$ is shifted to the longer wavelength: 408 nm. It is worth pointing out that the difference in the absorption energy between $[PtL_1Cl]^+$ and $[Pt(tpy)Cl]^+$ (∼60 meV) agrees very well with that in $E^{red(1)}$ between the two complexes (i.e., 50 meV). Therefore, the transition observed at around 400 nm can be assigned confidently to the MLCT transition.

The most important aspect into the absorption characteristics of the present Pt(II) complexes is the very large absorption intensity (molar absorptivity: ϵ) of $[PtL_1Cl]^+$ as compared with that of $[PtL_2Cl]^+$ or $[Pt(tpy)Cl]^+$ in the entire wavelength region observed. As seen in Figure 3b, tpy is transparent in the wavelength region longer than 330 nm,

Table 4. Spectroscopic and Excited-state Properties of the Pt(II) Complexes

compd	abs:[a] λ^{abs}/nm (ϵ/M^{-1} cm^{-1})	emission (298 K) λ^{em}/nm	Φ^{em}	$\tau^{em}/\mu s$	k_r/s^{-1}	k_{nr}/s^{-1}
$[Pt(tpy)Cl]^+$	402 (1800), 381, 349, 334, 318, 304, 283	Nd				
$[PtL_1Cl]^+$	408 (16 000), 386, 335, 288	550[b]	0.011[b]	0.6[b]	1.8×10^5	1.5×10^6
$[PtL_2Cl]^+$	404 (3500), 385, 333, 320 sh, 305 sh, 284	Nd				
L_1	318, 282					
L_2	332 sh, 315, 280					
[Pt-4'-ph-tpyCl]$^+$ [c]	402 (5200), 380 sh	535[d]	0.0021[d]	0.085[d]	2.5×10^4	1.2×10^7

[a] In acetonitrile. [b] In $CHCl_3$. [c] Data taken from ref 21. [d] In dichloromethane.

while the free L_1 and L_2 ligands show relatively strong absorption above 300 nm. Our previous studies on the spectroscopic properties of triarylborane derivatives indicate that the absorption band observed for L_1 or L_2 at around 320−350 nm is attributed to the electronic transition from the π(aryl) orbital to the vacant p-orbital on the boron atom (p(B)); π(aryl)−p(B) charge transfer,[5,6] where "aryl" would be mainly the phenyl-tpy unit in L_1 or L_2. Since the dihedral angle between the tpy and phenyl planes in L_1 is much smaller than that between the tpy and duryl planes as discussed above, the larger absorption intensity of the π-(aryl)−p(B) CT transition observed for L_1 as compared with that of L_2 will be the reasonable consequence in respect to the extent of electron delocalization in the ligand. Owing to such absorption characteristics of the free L_1 or L_2 ligand, both intraligand $\pi\pi^*$(tpy) and π(aryl)−p(B) CT transitions are superimposed in the absorption spectrum of $[PtL_1Cl]^+$ or $[PtL_2Cl]^+$ in the wavelength region shorter than 350 nm. Thus, the absorption intensities of $[PtL_1Cl]^+$ and $[PtL_2Cl]^+$ in this wavelength region can be explained roughly by those of the L_1 and L_2 ligands, respectively.

On the other hand, the molar absorption coefficient of the MLCT transition observed for $[PtL_1Cl]^+$ at λ^{abs} is 5 times larger than that of $[PtL_2Cl]^+$ (see Table 4), while the ratio of the ϵ value of the π(aryl)−p(B) CT transition in the free L_1 ligand to that in L_2 at around 320 nm is ∼1.5. It is well-known that the absorption strength of a molecule is determined by an oscillator strength (f) and the f value is given by

$$f = \left(\frac{8\pi m_e \tilde{\nu}}{3he^2}\right)\mu_e^2 \quad (1)$$

where m_e is the mass of an electron, $\tilde{\nu}$ is the energy of the transition, h is Planck's constant, and μ_e is the transition dipole moment.[44] For a given transition, a large absorption strength (ϵ) corresponds to a large transition dipole moment through the relation[44]

$$f \equiv 4.3 \times 10^{-9} \int \epsilon \, d\tilde{\nu} \quad (2)$$

The very large ϵ value for the MLCT transition of $[PtL_1Cl]^+$ as compared with that of $[PtL_2Cl]^+$ thus demonstrates the larger transition dipole moment of the former complex than that of the latter complex. This will be due to the contribution of the π(aryl)−p(B) CT to the MLCT transition in $[PtL_1Cl]^+$: synergetic effects of Pt(II)-to-L_1 MLCT and π(aryl)−p(B) CT (discussed later again). These results and discussions are consistent with the differences in the dihedral angle between the tpy and arylborane (phenyl or duryl) planes in the (L_1 or L_2) ligand as well as in the redox properties between $[PtL_1Cl]^+$ and $[PtL_2Cl]^+$ as described above.

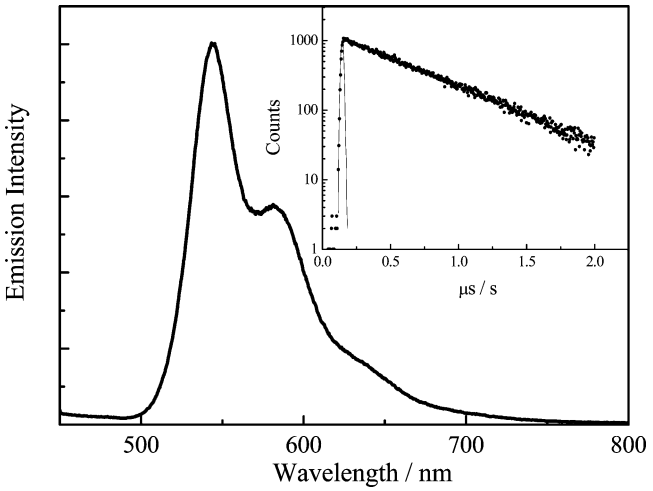

Figure 4. Emission spectrum of $[PtL_1Cl]^+$ (2×10^{-6} M) in $CHCl_3$ at 298 K (excitation wavelength = 400 nm). The inserted is the emission decay profile of the complex (monitored at 550 nm).

Emission Characteristics of $[PtL_1Cl]^+$. Among three Pt(II) complexes studied, only the $[PtL_1Cl]^+$ complex is emissive in solution at room temperature. The emission spectrum of $[PtL_1Cl]^+$ in $CHCl_3$ at 298 K is shown in Figure 4, in which the inserted figure displays the relevant emission decay profile. The emission data are included in Table 4. The $[PtL_1Cl]^+$ complex shows emission at the maximum wavelength (λ^{em}) of 550 nm with the lifetime (τ^{em}) and quantum yield (Φ^{em}) of 0.6 μs and 0.011, respectively. As an analogous complex to $[PtL_1Cl]^+$, it has been reported that $[Pt(ph\text{-}tpy)Cl]^+$ also shows room-temperature emission: λ^{em} = 535 nm, τ^{em} = 0.085 μs, and Φ^{em} = 0.0021 in CH_2Cl_2.[21] Thus, the Φ^{em} and τ^{em} values of $[PtL_1Cl]^+$ are larger and longer than the relevant value of $[Pt(ph\text{-}tpy)Cl]^+$ by factors of 7 and 5, respectively. The data indicate that the radiative (k_r) and nonradiative decay rate constants (k_{nr}) of $[PtL_1Cl]^+$ are 1.8×10^5 and 1.5×10^6 s^{-1}, respectively, while those of $[Pt(ph\text{-}tpy)Cl]^+$ are 2.5×10^4 and 1.2×10^7 s^{-1}, respectively (see Table 4). These values demonstrate that an introduction of the dimesitylborane group to the ph-tpy ligand gives rise to an increase in k_r by 7 times, while the

(44) Turro, N. J. *Modern Molecular Photochemistry*; Benjamin/Cummings Publishing: Menlo Park, NJ, 1978.

k_{nr} value of $[PtL_1Cl]^+$ becomes almost 1/10 of the value for $[Pt(ph\text{-}tpy)Cl]^+$.

It is known that k_r of a molecule is related to the oscillator strength of the relevant absorption transition and, thus, to the ϵ value:

$$k_r \approx \tilde{\nu}^2 f \approx \tilde{\nu} \int \epsilon \, d\tilde{\nu} \quad (3)$$

The large k_r value observed for $[PtL_1Cl]^+$ agrees very well with the larger ϵ (MLCT) value of $[PtL_1Cl]^+$ (1.6×10^4 M^{-1} cm^{-1}) as compared with that of $[Pt(ph\text{-}tpy)Cl]^+$ (5.2×10^3 M^{-1} cm^{-1}), which is ascribed essentially to the enhanced absorption-transition dipole moment by the synergetic effects between the Pt(II)-to-L_1 MLCT and π(aryl)−p(B) CT interactions. Such synergetic interactions in the complex should stabilize the MLCT excited-state energy. In practice, the emission spectrum of $[PtL_1Cl]^+$ ($\lambda^{em} = 550$ nm) is shifted to the longer wavelength as compared with that of $[Pt(ph\text{-}tpy)Cl]^+$ ($\lambda^{em} = 535$ nm). The X-ray crystal structure of $[PtL_1Cl]^+$ is very similar to that of $[Pt(ph\text{-}tpy)Cl]^+$, except for the presence or absence of the dimesitylborane group. This indicates that the coordination structures around the Pt(II) ions in these complexes are very similar and, thus, the d−d excited-state energy will be comparable between the two complexes. Since nonradiative decay from the excited state of a Pt(II) complex proceeds via thermal population from the emissive MLCT excited-triplet state to the higher lying excited d−d triplet state, the lower MLCT excited-state energy of $[PtL_1Cl]^+$ as compared with that of $[Pt(ph\text{-}tpy)Cl]^+$ results in the decrease in the k_{nr} value of the former complex. The strong and long-lifetime emission of $[PtL_1Cl]^+$ is thus explained reasonably by the synergetic MLCT and π(aryl)−p(B) CT interactions.

It should be noted that clear evidence for the participation of the π(aryl)−p(B) CT interactions in the MLCT excited state of $[PtL_1Cl]^+$ has been obtained. It has been reported that the vacant p-orbital on the boron atom in a triarylborane derivative coordinates selectively with a fluoride ion and this gives rise to the changes in both absorption and emission spectra of the derivative.[1,3,4] For example, the binding constant of TAB with a fluoride ion in THF has been reported to be 10^5 M^{-1}, while other halide ion such as Cl^- or Br^- cannot bind with TAB. Similar to such observations on TAB, an addition of a fluoride ion (i.e., tetra-*n*-butylammonium fluoride: (TBA)F) in a $CHCl_3$ solution of $[PtL_1Cl]^+$ results in quenching of the MLCT emission without any appreciable change in the spectral band shape: Figure 5. Furthermore, emission quenching of $[PtL_1Cl]^+$ by F^- accompanies a double exponential emission decay: the short- (τ_s) and long-lifetime components (τ_l) of 40−50 ns and ∼0.5 μs, respectively. The τ_s value is very similar to the emission lifetime of $[Pt(ph\text{-}tpy)Cl]^+$ (80 ns),[21] while the τ_l value is comparable to that of $[PtL_1Cl]^+$ in the absence of F^- (0.6 μs). It is worth nothing that although the τ_s and τ_l values are almost constant irrespective of the concentration of a fluoride ion ($[F^-]$), the contribution of the τ_s component to the overall decay profile increases with increasing $[F^-]$ (data are not shown here). This indicates that the τ_s component observed in the presence of F^- is attributed to the excited $[PtL_1Cl]^+$ complex coordinated with a fluoride ion. Although the effect of a fluoride ion on the absorption spectrum of $[PtL_1Cl]^+$ is rather small, MLCT emission quenching of the complex by F^- in Figure 5 demonstrates clearly the participation of the π(aryl)−p(B) CT interactions in the MLCT excited state of $[PtL_1Cl]^+$. Therefore, we conclude that the excited state of the $[PtL_1Cl]^+$ complex is best characterized by the MLCT and π(aryl)−p(B) CT interactions.

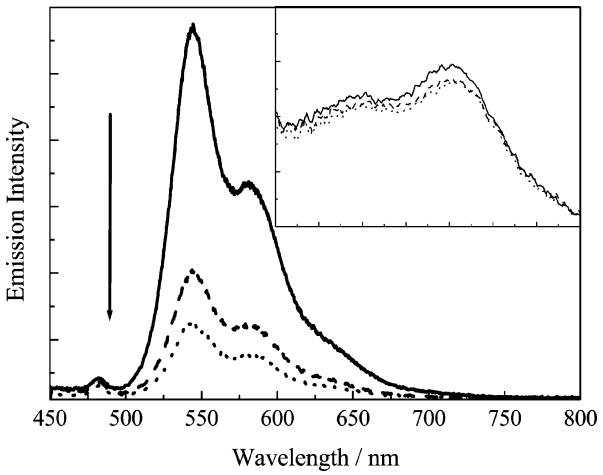

Figure 5. Emission quenching of $[PtL_1Cl]^+$ by a fluoride ion ((TBA)F) in $CHCl_3$ at 298 K (excitation wavelength = 400 nm). The insert is the relevant absorption spectrum changes of the complex. $[PtL_1Cl]^+ = 1.0 \times 10^{-6}$ M, and [TBAF] = 0 (solid line), 1.1×10^{-6} (dashed line), and 2.2×10^{-6} M (dotted line).

All of the experimental results on the redox, spectroscopic, and excited-state properties of $[PtL_1Cl]^+$ are explained reasonably by a single context of the participation of the π(aryl)−p(B) CT interaction in the MLCT excited state. Also, the non- or very weak emissive nature of the $[PtL_2Cl]^+$ complex at ambient temperature can be explained by weak coupling between the MLCT and π(aryl)−p(B) CT states.

Conclusions

This study demonstrated that the synergetic Pt(II)-to-L_1 MLCT and π(aryl = L_1)−p(B) CT interactions determined the redox, spectroscopic, and excited-state properties of $[PtL_1Cl]^+$. Owing to such interactions, $[PtL_1Cl]^+$ shows strong room-temperature emission with $\Phi^{em} = 0.011$ and $\tau^{em} = 0.6$ μs, which are considerably larger and longer, respectively, than the relevant value of other Pt(II) complex having a tpy-type ligand. The importance of the electron communication between the Pt(II) ion and p(B) through the MLCT/π(aryl)−p(B) CT interactions in determining the excited-state properties of the Pt(II) complex is supported by almost nonemissive nature of the $[PtL_2Cl]^+$ complex, in which the large dihedral angle between the tpy and duryl(dimesitylborane) groups disturbs electron delocalization over the ligand. Phenomenologically, the present results on $[PtL_1Cl]^+$ are very similar to the effects of π-conjugation in the tpy ligand on the photophysical properties of a Ru(II) complex having a 4′-

(2-pyrimidyl)terpyridine ligand.[45−49] Another important aspect of this study is the enhanced transition dipole moment of MLCT absorption, as revealed by the large ϵ value of the MLCT absorption band of $[PtL_1Cl]^+$ as compared with that of $[Pt(tpy)Cl]^+$ or $[Pt(ph\text{-}tpy)Cl]^+$. Although we have not determined the dipole moment in the MLCT excited state of $[PtL_1Cl]^+$, the value should be much larger than that of $[Pt(tpy)Cl]^+$ or $[Pt(ph\text{-}tpy)Cl]^+$. Since all of the present results can be explained reasonably by the participation of the synergetic MLCT/π(aryl)−p(B) CT interactions in $[PtL_1Cl]^+$, strongly emitting transition metal complexes could be realized through appropriate design of a boron-conjugated π-chromophore ligand. It is worth noting, finally, that the effects of synergetic MLCT and π(aryl)−p(B) CT interactions on the redox, spectroscopic, and excited-state properties of a transition metal complex will not be limited to those of a Pt(II) complex and the present L_1/L_2 ligands. The present idea of the synergetic MLCT/π(aryl)−p(B) CT effects on the electronic structure of a compound could be applied to various transition metal complexes with a variety of π-chromophoric ligands.

(45) Fang, Y.-Q.; Taylor, N. J.; Hanan, G. S.; Loiseau, F.; Passalacqua, R.; Campagna, S.; Nierengarten, H.; Dorsselaer, A. V. *J. Am. Chem. Soc.* **2002**, *124*, 7912.
(46) Polson, M. I. J.; Taylor, N. J.; Hanan, G. S. *Chem. Commun.* **2002**, 1356.
(47) Polson, M. I. J.; Medlycott, E. A.; Hanan, G. S.; Mikelsons, L.; Taylor, N. J.; Watanabe, M.; Tanaka, Y.; Loiseau, F.; Passalacqua, R.; Campagna, S. *Chem.*—Eur. J. **2004**, *10*, 3640.
(48) Passalacqua, R.; Loiseau, F.; Campagna, S.; Fang, Y.-Q.; Hanan, G. S. *Angew. Chem., Int. Ed.* **2003**, *42*, 1607.
(49) Medlycott, E. A.; Hanan, G. S. *Chem. Soc. Rev.* **2005**, *34*, 133.

Acknowledgment. We thank Prof. Y. Sasaki and Dr. K. Tsuge at the Division of Chemistry, Hokkaido University, for X-ray crystallography experiments.

IC061435B